

CHARACTERIZATION OF A RADIO FREQUENCY SPACE ENVIRONMENT PATH EMULATOR FOR EVALUATING SPACECRAFT RANGING HARDWARE*

Jason W. Mitchell[†], Philip J. Baldwin[‡], Brent W. Barbee[§]
Emergent Space Technologies, Inc., Greenbelt, MD 20770-6334, USA

Rishi Kurichh[¶], and Richard J. Luquette^{||}
NASA Goddard Space Flight Center, Greenbelt, MD 20771, USA

Abstract

Development of the Path Emulator for Radio Frequency Systems (PERFS) continues at the National Aeronautics and Space Administration (NASA) Goddard Space Flight Center (GSFC). PERFS enables realistic simulations, which require S-band Radio Frequency (RF) ranging sensors for relative navigation, by accurately emulating the dynamic environment through which the RF signals travel. Dynamic environments include effects of the medium, moving platforms, and radiated power. PERFS is an essential component of the NASA GSFC Formation Flying Testbed (FFTb) for hardware-in-the-loop testing of the Inter-spacecraft Ranging and Alarm System (IRAS) for the Magnetospheric Multiscale (MMS) mission. The function and performance of the first production PERFS are presented.

Keywords: radio frequency signals, spacecraft crosslinks, relative navigation, delay, signal modulation, real-time, hardware-in-the-loop, formation flying.

Acronyms

ADC	Analog-to-Digital Converter
CCS	Crosslink Channel Simulator
CoM	Center of Mass
DAC	Digital-to-Analog Converter
DDS	Direct Digital Synthesizer
DSA	Digital Step Attenuator
R_{\oplus}	Earth Radii
ESA	European Space Agency

*This material is declared a work of the U.S. Government and is not subject to copyright protection in the United States.

[†]Aerospace Scientist, jason.mitchell@emergentspace.com, AIAA Senior Member.

[‡]Assoc. Software Engineer, philip.baldwin@emergentspace.com.

[§]Aerospace Engineer, brent.barbee@emergentspace.com.

[¶]Computer Engineer, Code 596, rishi.kurichh-1@nasa.gov.

^{||}Aerospace Engineer, Project PI, Code 591, rich DOT luquette AT nasa DOT gov, AIAA Member.

FFTB	Formation Flying Testbed
FOV	Field of View
FPGA	Field Programmable Gate Array
FSL	Free Space Loss
GEONS	GPS Enhanced On-Board Navigation System
GN&C	Guidance, Navigation & Control
GPS	Global Positioning System
GSFC	Goddard Space Flight Center
IF	Intermediate Frequency
IRAS	Inter-spacecraft Ranging and Alarm System
LOS	Line of Sight
MMS	Magnetospheric Multiscale
NASA	National Aeronautics and Space Administration
PCC	PERFS Command Client
PERFS	Path Emulator for Radio Frequency Systems
PRN	Pseudo-Random Noise
RF	Radio Frequency
RX	Receive
s/c	spacecraft
SI	Stellar Imager
SPECS	Submillimeter Probe of the Evolution of Cosmic Structure
TRL	Technology Readiness Level
TX	Transmit
USB	Universal Serial Bus
USRP	Universal Software Radio Peripheral
VCP	Virtual COM Port
XES	Crosslink (X/L) Environment Simulator
X/L	Crosslink
YIG	Yttrium Iron Garnet

I. Introduction

Both the National Aeronautics and Space Administration (NASA) and the European Space Agency (ESA) are evaluating formation flying concepts for numerous missions. A brief list of current missions include, NASA: Magnetospheric Multiscale (MMS),¹ Black Hole Imager,^{2,3} Submillimeter Probe of the Evolution of Cosmic Structure (SPECS),⁴ Stellar Imager (SI),⁵ ESA: Darwin,⁶ Prisma,⁷ Proba-3.⁸

The Formation Flying Testbed (FFTB)⁹⁻¹¹ at NASA Goddard Space Flight Center (GSFC) provides a unique environment for designing and testing formation flying Guidance, Navigation & Control (GN&C) algorithms. The FFTB enables end-to-end capability for testing GN&C algorithms in real-time, and in the presence of essential flight hardware, e.g. relative navigation sensors and crosslink transceivers. By including this hardware directly in the closed-loop testing, researchers and engineers gain valuable information about the interaction and performance of their algorithms and essential hardware.

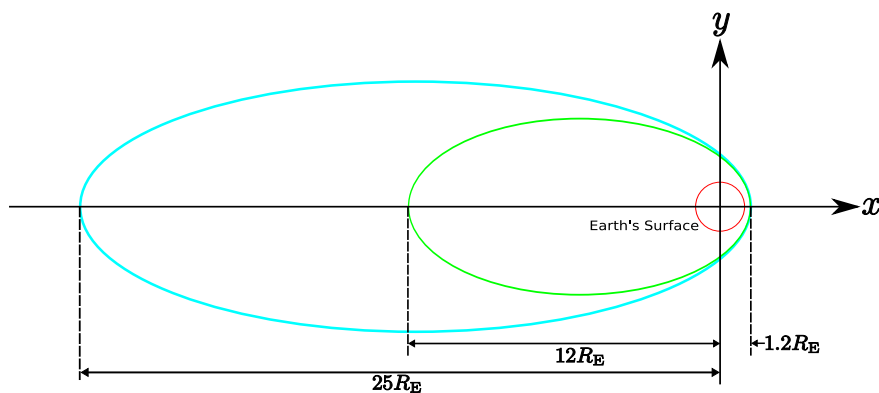


Figure 1. Range of MMS orbit phases.

In support of the MMS mission, NASA GSFC is maturing the Inter-spacecraft Ranging and Alarm System (IRAS) to Technology Readiness Level (TRL) 6**.^{12,13} The MMS mission, composed of a four satellite formation, is currently scheduled for launch in 2014. The formation will progress through a variety of highly eccentric orbits with perigee altitude of approximately 1.2 Earth Radii (R_{\oplus}), and apogee altitude between $12 R_{\oplus}$ to $25 R_{\oplus}$, Figure 1, depending on mission phase.¹⁴ The IRAS serves a number of critical roles for this mission, including: Global Positioning System (GPS) and crosslink ranging; on-board absolute and relative orbit determination using the GPS Enhanced On-Board Navigation System (GEONS);¹⁵ crosslink communications for navigation information sharing; and science alarm messaging.

The core capabilities of the FFTB, as a platform for testing critical hardware and software algorithms in-the-loop, have expanded to include S-band Radio Frequency (RF) modems for inter-spacecraft communication and ranging. To enable realistic simulations that require RF ranging sensors for relative navigation, a mechanism is needed to buffer the RF signals exchanged between spacecraft that accurately emulates the dynamic environment through which those signals travel. Dynamic environments include the effects of the medium, moving platforms, and radiated power.

In previous work, Hunt et al.¹⁶ describe a Crosslink Channel Simulator (CCS). This device was successfully integrated into the FFTB and provides a single, dynamic, bi-directional RF path between two spacecraft. Mitchell and Luquette¹¹ and Mitchell et al.¹⁷ describe two spacecraft scenarios in which the CCS was the communication medium via hardware crosslinks. In these scenarios, the hardware crosslinks were used to exchange data between spacecraft, e.g. pseudorange and simulated range measurements, however no direct RF ranging was performed using hardware crosslinks.

Since the MMS mission is composed of four spacecraft, each with multiple antennas, the IRAS TRL 6 testing in the FFTB will require multiple bi-directional channels. The Path Emulator for Radio Frequency Systems (PERFS), currently under development at NASA GSFC, will provide this additional RF channel capacity. Each PERFS device will provide a single, dynamic, bi-directional, RF path between two spacecraft, much like the CCS. However, the PERFS will have a smaller footprint and lower cost than the CCS, and

**TRL 6 represents a successful system or subsystem model or prototype demonstration in a relevant environment.

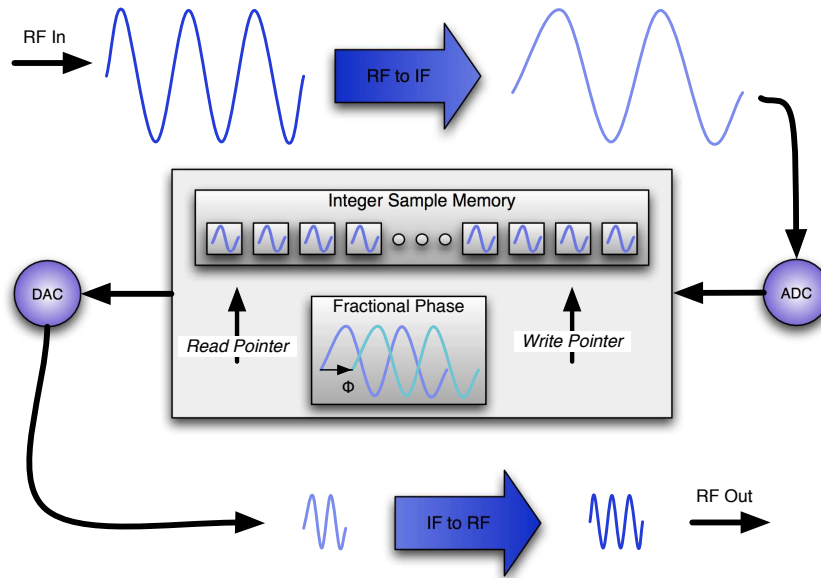


Figure 2. PERFS internal concept of operations.

provide additional testing flexibility. Mitchell et al.¹⁸ presented the efficacy of a PERFS proof-of-concept and described its performance in relation to MMS ranging requirements. In the following, we review the design concept and present the performance analysis of the production PERFS.

II. Design

PERFS was designed to dynamically modulate RF signals by applying delay, Doppler, and attenuation that accurately emulates the space environment. The following sections review the concept of operation of PERFS, discuss commanding and environment models, and introduce the notion of a PERFS network.

II.A. Concept

In transitioning from prototype to production, the PERFS concept of operations remains the same, Figure 2. Flowing from top-left to bottom-right, the S-band RF center frequency input is down-converted to the Intermediate Frequency (IF) of 35.42 MHz. The IF is sampled by the Analog-to-Digital Converter (ADC). The parameters that specify Doppler shift and delay are applied. The sample memory provides the integer delay, and the Direct Digital Synthesizer (DDS) generates the fractionally delayed and Doppler shifted signal that is converted to analog via the Digital-to-Analog Converter (DAC). Digital Step Attenuators (DSAs) provide the commanded attenuation to the IF signal. Finally, the IF signal is up-converted to RF. Additional information about specific operations, highlighted in Figure 2, follow:

IF SAMPLING: The IF input is digitized with a 12-bit ADC running at 100 MSPS, as driven by the write-pointer DDS.

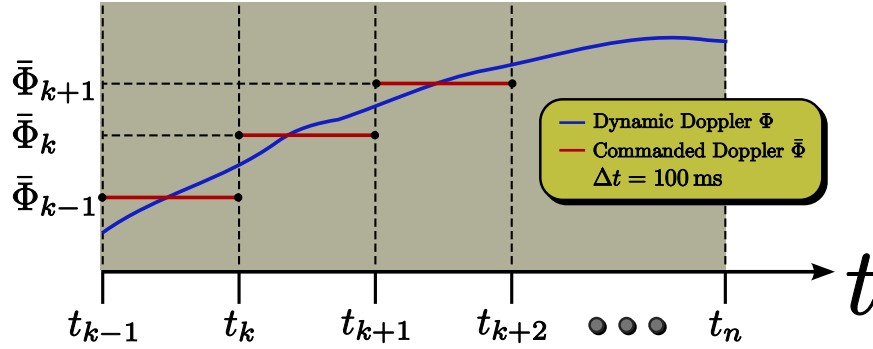


Figure 3. PERFS implementation of constant Doppler over a simulation interval.

SAMPLE MEMORY: The ADC output is provided to a Field Programmable Gate Array (FPGA) that implements a circular memory buffer. Each integer sample in the memory buffer represents 10 ns of delay based on the 100 MHz DDS clocks when no Doppler is applied.

DOPPLER AND DELAY: The Doppler shift is generated by varying the frequency of the read-pointer DDS clock output. The total instantaneous delay is a combination of the integer and fractional delay. The integer delay is provided by sample memory, while the fractional delay is represented by the phase difference between DDS clocks.

ATTENUATION: Attenuation is applied via DSA in 0.5 dB steps, which are controlled by the FPGA. The applied attenuation includes free space loss, antenna gain and alignment, etc., as provided in the commanded parameters. The current configuration of PERFS is limited to a maximum range of approximately 3500 km.

II.B. Commanding and Environment Modeling

The PERFS Command Client (PCC) is responsible for providing PERFS with the real-time data necessary to properly model the RF environment between transmitting and receiving crosslink antennas. For open-loop MMS IRAS testing, all trajectory information is known *a priori*. This simplifies the PCC design considerably, as there is no need to compute channel parameters in real-time. Rather, the trajectory information can be processed prior to any run, and the necessary delay, Doppler, and attenuation can be read from a data file. However, the PCC must still receive this data in real-time. The PCC design then requires only:

- a) the ability to compute and tabulate delay, Doppler, and attenuation from truth trajectory (orbit and attitude) files and antenna gain files; and
- b) the ability to read the delay, Doppler, and attenuation data and command the PERFS in real-time as the simulation unfolds.

PERFS receives channel parameter data via Universal Serial Bus (USB) version 2 every 100 ms, as shown in Figure 3. Channel parameters received at t_k will be implemented at t_{k+1} . Over the 100 ms interval, the Doppler is held constant. As a result, when commanding parameters driven by simulation physics, it is best to command parameters that represent the best average error over the interval. These best average parameters should consider all modeling errors.

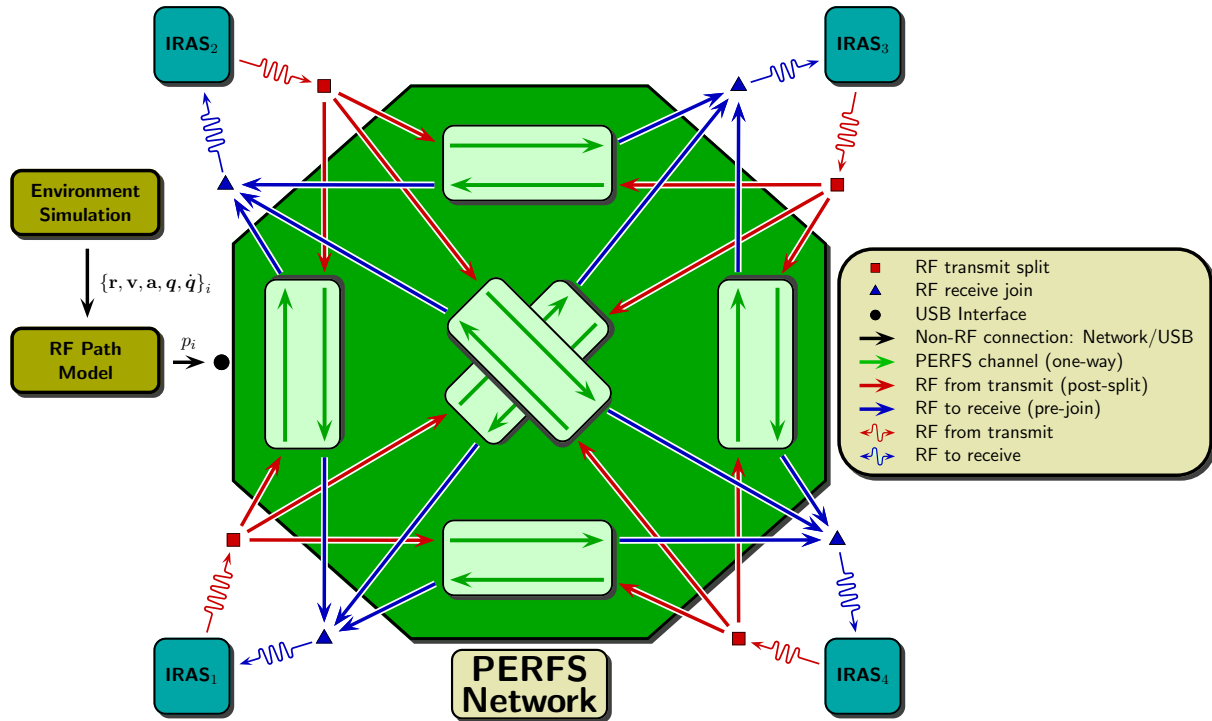


Figure 4. PERFS network connectivity for IRAS testing.

The environment modeling software, called the Crosslink (X/L) Environment Simulator (XES), is written in C, and computes the requisite RF channel parameters for an arbitrary number of spacecraft, each with an arbitrary number of transmitters and receivers. XES is given translational and rotational ephemerides for all spacecraft, as well as antenna modeling parameters for all spacecraft antennas. At each time-step, XES outputs the instantaneous RF environment parameters for each possible transmission path, i.e. transmit antenna to receive antenna, whenever a Line of Sight (LOS) exists, and received signal power is sufficient. XES is capable of running in batch mode to generate all data *a priori* or in real-time mode, sequence by sequence. As previously mentioned, batch mode is sufficient for the open-loop MMS mission simulations. The real-time operational mode allows for closed-loop control with hardware-in-the-loop simulations, and thus facilitates future work.

II.C. PERFS Network

The MMS mission consists of four (4) identical spacecraft each equipped with an IRAS. IRAS allows an individual spacecraft to communicate with its three (3) neighbors, Figure 4. Thus, for ground testing and simulation of the complete system, six (6) total bi-directional paths are necessary to enable communication between any single spacecraft and each of the remaining three (3) spacecraft.

To accurately simulate this space RF environment, a system or network of RF emulators are needed to model attenuation, delay, and Doppler.

A single PERFS unit provides the ability to simulate a single space RF link between two spacecraft. A network of PERFS units allows for the simulation of multiple RF links between multiple spacecraft. In a constellation scenario, each PERFS unit represents one RF link be-

tween two spacecraft, i.e. transmit and receive pair. A four (4) spacecraft formation requires 6 PERFS units to simulate full RF connectivity. The number of units needed is determined by the number of transmitters, receivers, and/or transceivers. For our investigation, we identify two (2) distinct spacecraft configurations:

1. Each spacecraft carries some number of transmitters and receivers, and no transceivers;
2. Each spacecraft carries zero or more transceivers, transmitters, and receivers;

where Configuration 1 appears as special case of Configuration 2.

For Configuration 1, it is straightforward to determine that the total number of PERFS units required is given by

$$P = \sum_{k=1}^S \sum_{l=1, l \neq k}^S T_k R_l, \quad (1)$$

where P is the total number of PERFS units, S is the total number of spacecraft, T_k is the number of transmitters on spacecraft k spacecraft, and R_l is the number of receivers on spacecraft l spacecraft. In the general case of Configuration 2, the total number of PERFS units needed is given by

$$P = \sum_{k=1}^S \sum_{l=1, l \neq k}^S [(X_k + T_k)R_l + T_k X_l] + \sum_{k=1}^{S-1} \sum_{l=1, l > k}^S X_k X_l, \quad (2)$$

where P, S, T_k and R_l are as in Eq. 1, and X_j is the number of transceivers on spacecraft j .

The PERFS network is implemented as an aggregation of individual PERFS units, each with a separate, but coordinated command client. The network enables simulation of rotating spacecraft by coordinating the XES output with the proper PCC. As a specific Transmit (TX)-Receive (RX) link is broken, XES informs the PCC for that link to maximally attenuate the signal. This effectively severs the RF link between the antennae, thus establishing the coherent network function.

III. RF Modeling

RF path data is provided to the PCC by the Crosslink (X/L) Environment Simulator (XES), a computer program written in support of PERFS and whose purpose is to model the RF signal delay (Δt), Doppler shift (Δf), and attenuation (A) on a per-RF path basis between two or more spacecraft (s/c).

III.A. Assumptions and Limitations

The s/c are assumed to all be moving about a central body and rotating arbitrarily about their nominal Center of Mass (CoM) locations, as shown in Figure 7. Each s/c may have various numbers of RX and TX antennae mounted on it, each with a gain pattern that is symmetric about the antenna boresight. Antenna geometry is shown in Figure 5. The relative kinematics between each combination of RX and TX antennae is accounted for, and azimuthal and elevational antenna FOV constraints can be specified on a per-antenna basis, as seen in Figure 6.

At its current phase of development, XES contains some particular simplifying assumptions that may limit its accuracy in certain scenarios. These are:

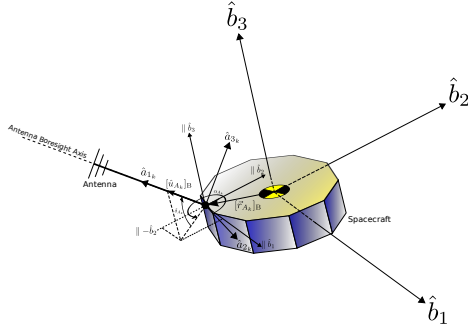


Figure 5. Antenna geometry in the spacecraft body frame.

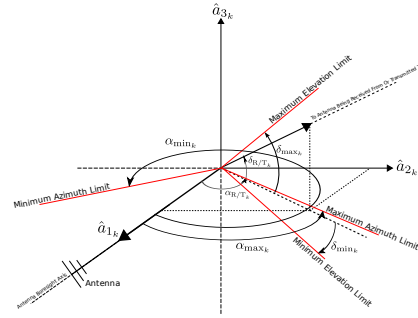


Figure 6. Geometry for antenna FOV limits relative to boresight.

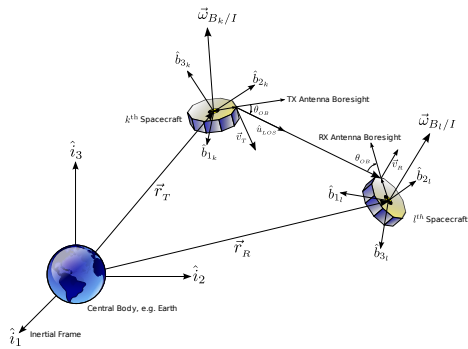


Figure 7. Relative spacecraft geometry.

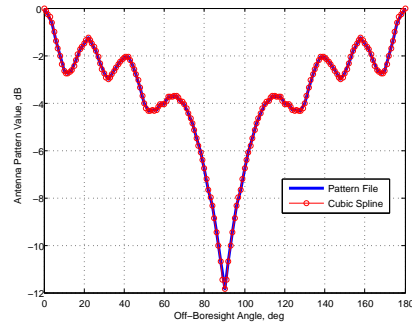


Figure 8. Sample antenna pattern with cubic spline interpolation.

- The spacecraft have an instantaneously static relative geometry for the purposes of calculating signal delay and Free Space Loss (FSL) at every time step;
- the ionosphere and troposphere are not modeled;
- signal multipath effects are not modeled.

XES computes the instantaneous relative velocity and geometric range rate between each combination of TX and RX antennae at each of the times provided in the input orbit and attitude ephemeris files. The instantaneous range rates are used to compute the received signal Doppler shifts, but that is the extent to which the spacecraft relative motion is considered.

In reality, the relative geometry between RX and TX antennae on the spacecraft changes between the time at which a signal is transmitted and when it is received, since RF signals are constrained to travel at light speed. Additional calculations would be required to determine the actual signal delay and the actual distance between the TX and RX points for the purposes of computing FSL. The time values output by XES should be for the actual times of signal reception, but instead they are simply the input ephemeris time values.

When the range rates between the RX and TX antennae are sufficiently smaller than light speed and when the geometric ranges are small enough that the spacecraft cannot move appreciably before the RF signals cross the distances at light speed, the errors caused by the above assumptions are small and may not be significant enough to matter for the user's purposes.

III.B. Signal Delay

The delay between the transmission and reception of an RF signal is equal to the time required by the signal to propagate between the transmitter and the receiver, given as¹⁹

$$\Delta t = \frac{\rho}{c} \quad (3)$$

where Δt is the inertial coordinate time, ρ is the geometric range, and $c = 299,792,458.0$ m/s is the speed of light in a vacuum.²⁰

III.C. Signal Doppler Shift

An RF signal exchanged between two spacecraft is subject to classical and relativistic effects, causing the RX signal frequency to differ from the TX frequency according to

$$f_R = f_T + \Delta f \quad (4)$$

where f_R is the RX signal frequency, f_T is the TX signal frequency, and Δf is the Doppler shift, all in units of Hz. For the purposes of modeling the RF environment, f_T is known *a priori* and therefore Δf is computed as a function of f_T , among other things.

The relativistic effects on RF signal frequency are due primarily to the facts that there is typically significant relative motion between spacecraft and that there are often significant differences in spacecraft altitudes with respect to the central body. The consequence of the former is classical Doppler shift with relativistic corrections, while the consequence of the latter, also due to relativity and often referred to as gravitational redshift in the literature, is due to the fact that while gravity cannot change the speed of light, a gravity field can do work on light to change its energy, which correspondingly changes its frequency.²¹

After derivation that is omitted here for brevity, the total relativistic Doppler shift, retaining terms through order v^2/c^2 , is²²

$$\Delta f = f_T \left(-\frac{\dot{\rho}}{c} \left(1 + \frac{\hat{u}_{LOS} \cdot \vec{v}_T}{c} \right) + \frac{\mu}{c^2} \left(\frac{1}{r_R} - \frac{1}{r_T} \right) + \frac{v_R^2 - v_T^2}{2c^2} \right) \quad (5)$$

where $\dot{\rho}$ is the geometric range rate in m/s, \hat{u}_{LOS} is the LOS unit vector pointing from RX to TX antenna, μ is the gravitational parameter of the central body in units of m^3/s^2 , and r_R , v_R , r_T , and v_T are the RX and TX antenna inertial position and velocity vector magnitudes in units of m and m/s, respectively.

III.D. Signal Attenuation

The equation for FSL, in units of dB, used within XES is

$$L_{FS} = 20 \log_{10} \left(\frac{4\pi}{c} \rho f_T \right) \quad (6)$$

and is a function of the geometric range between TX and RX antenna and the transmit frequency. Eq. (6) was obtained by analysis of material presented in [19, 23].

At the beginning of each unique RF path is a TX antenna and at the end is a RX antenna. Each antenna has a gain pattern associated with it that specifies how it modifies the signal as a function of off-boresight angle, θ_{OB} , which spans the range of $[0, \pi]$ radians. The RX

	Min	Max	Resolution
Attenuation	90 dB	0 dB	0.5 dB
Range	250 m	3500 km	5 cm
Doppler	0 Hz	5 kHz	10 mHz

Table 1. PERFS performance indicators.

antenna gain is denoted as G_R and the TX antenna gain is denoted as G_T ; both are in units of dB.

The total signal attenuation in dB for an RF path is equal to the FSL attenuation minus the RX gain, the TX gain, and an arbitrary constant user-specified gain, G (dB) as shown in Eq. (7). XES always outputs total signal attenuation, A , as a positive quantity unless the gains of the RX and TX antennae and the arbitrary user-specified gain are all together sufficient to completely overcome FSL.

$$A = L_{FS} - G_R - G_T - G \quad (7)$$

III.D.1. Antenna Modeling

Antenna pattern data is provided to XES in the form of antenna pattern files, which contain a table of off-boresight angle values and corresponding antenna gain values. A bisection method table search algorithm, which converges in $\mathcal{O}(\log_2 n)$ tries,²⁴ is used in conjunction with a cubic spline interpolation algorithm²⁴ to determine antenna gain values for arbitrary off-boresight angles, as shown in Figure 8.

IV. Test Descriptions

Due to limitations of hardware availability and recent requirement changes, the following tests were completed to best evaluate the current state of PERFS with respect to the performance indicators shown in Table 1. These tests focus largely on Doppler control, Doppler resolution and error^{††}.

- Sideband Suppression
 - Filtering of Spurious Signals
- Doppler
 - Commanded vs. Measured
 - Minimum Resolution
 - Maximum Doppler Capability
 - Carrier Tracking
 - Code Tracking
- Delay
 - Electrical Path Delay/Minimum Range Offset
- USB Interface

^{††}At this time, recently discovered implementation issues associated with sideband suppression, attenuation, and phase resolution are being addressed.

- Data Throughput

These tests are described in more detail below.

SIDEBAND SUPPRESSION: Signal products resulting from mixing must not interfere with the center frequency of interest. To determine the sideband suppression, an RF sine wave is input to the PERFS and the output sideband peak power is measured.

COMMANDED VS. MEASURED DOPPLER: This test illustrates the Doppler control precision. A sequence of Doppler values, ranging from 0 Hz to 10 kHz, is commanded and recorded 50 times. The data is post-processed to determine the error.

MAXIMUM DOPPLER: The bandwidth specification for PERFS is 20 MHz. This test determines the maximum amount of Doppler that can be applied.

CARRIER/CODE TRACKING This test evaluates the ability of PERFS to maintain coded signal integrity during Doppler steps. A software GPS receiver^{25,26} is used to track GPS Pseudo-Random Noise (PRN) 1 coded onto the S-band carrier during a Doppler ramp of 30 Hz/s for a duration of 5 min.

ELECTRICAL PATH DELAY: Using a network analyzer this test determines the minimum delay through PERFS. The electrical path delay tells us the minimum range that can be modeled with PERFS. The theoretical limit of range control is a single 10 ns sample. However, this does not account for delay through filters, and other RF components.

DATA THROUGHPUT: Current estimates require that command and telemetry maintain a total data rate of not less than 5 KB/s, with a nominal 100 ms update rate. There are several driver options available for communicating with the FTDI chipset in Linux, including the Virtual COM Port (VCP) drivers²⁷ found in the default Linux kernel v2.6 via the `ftdi_sio` library, and PERFS uses this default driver. In this test, a default 128 byte command buffer is written to the device and a 64 byte simulated telemetry result is read into local buffer. This is done repeatedly over various time intervals to establish a baseline data rate.

V. Results

The tests described in the previous section continue to be performed incrementally and repeated during PERFS development. This approach has provided feedback and directed debugging efforts of the first production build.

V.A. Sideband Suppression

Figure 9 shows that in an initial configuration, the first sideband frequency was approximately 35.2 MHz and 9 dB below the nominal center frequency. This value is outside the specified 20 MHz span, but is not 50 dB below the strongest desired signal component, as required. After examining the RF front-end design, it was determined that the placement of the Yttrium Iron Garnet (YIG) filters in relation to the RF DSAs resulted in the reduced attenuation.

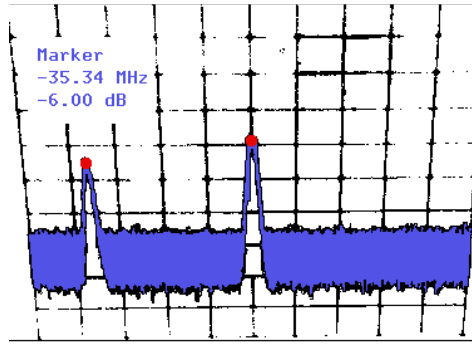


Figure 9. Side-band suppression of highest mixing multiple.

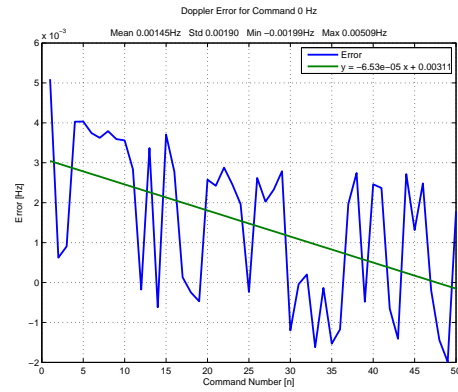


Figure 10. Baseline 0 Hz pass-thru.

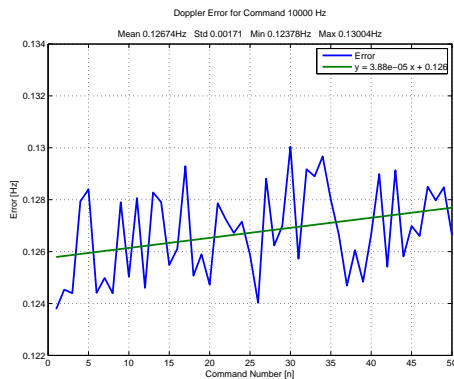


Figure 11. Commanded vs. measured Doppler: 10 kHz.

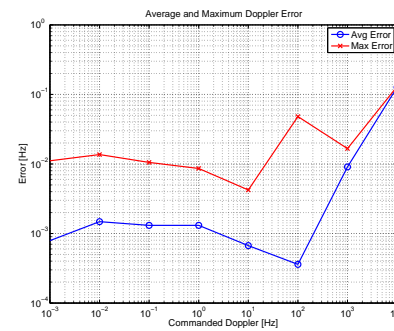


Figure 12. Average and maximum deviations from commanded Doppler.

V.B. Doppler

Figure 10 shows the 0 Hz commanded Doppler baseline, which establishes a pass-thru resolution of approximately 3 mHz. The Doppler sequence of 1 mHz, 10 mHz, 100 mHz, 1 Hz, 10 Hz, 1 kHz, and 10 kHz were each commanded and measured 50 times. A summary of the average and maximum deviations in the commanded sequence is given in Figure 12.

From 0 Hz to 1 kHz, the average Doppler error remained below 10 mHz. However, with the largest Doppler value, an average and maximum error of 126 mHz and 130 mHz, respectively, was observed, see Figure 11. Although this exceeds the requirement of 10 mHz, the resulting error is a small fraction of the total Doppler value commanded. Despite this, over the significant range of Doppler values commanded, the test was successful.

An additional test performed examined the maximum amount of Doppler that could be commanded. By observing a range of values between 25 MHz to 27 MHz, the maximum Doppler value appeared to be below 27 MHz; at 29 MHz the measured value deviated by 5 Hz, while at 27 MHz, the measured value deviated by approximately 200 Hz. Since the specified bandwidth is 20 MHz, it is expected that the maximum Doppler requirement will be met, however further testing is required to determine a more precise value.

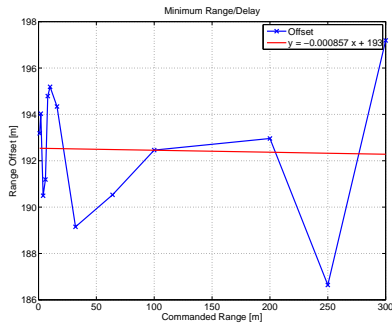


Figure 13. Range offset.

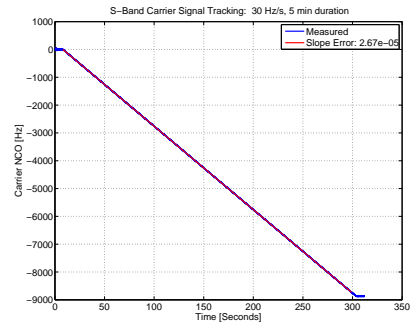


Figure 14. S-band carrier tracking for 30 Hz/s.

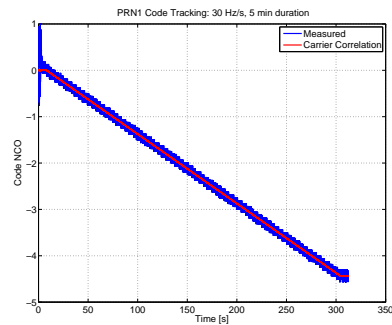


Figure 15. Code tracking (PRN 1) for commanded 30 Hz/s.

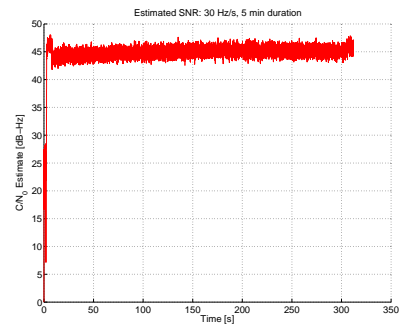


Figure 16. Estimated C/N_0 for 30 Hz/s.

V.C. Electrical Delay

The electrical delay through PERFS was measured using an HP network analyzer. This method provides a measurement accuracy of approximately 0.5 m. PERFS requires at least a one sample separation in the sample memory buffer before values can be reliably used—One 10 ns sample contains 3 m of carrier signal. Theoretically, this is the minimum range value, however the additional circuitry and RF components must be considered. Figure 13 shows the range offset for a given commanded range value. The fitted value indicates a range offset, or path delay, of approximately 193 m or 640 ns. From Figure 13, it is clear that there is considerable noise in the measurement.

V.D. Carrier/Code Tracking

This test ensures that modulated data are not corrupted by PERFS. Recorded signal data is post-processed with a software GPS receiver^{25,26} to determine the efficacy of passing carrier encoded data through PERFS. A summary of the test results is shown in Figures 14–16.

Figure 14 shows that the S-band carrier frequency is tracked through the -30 Hz/s Doppler ramp, with a fitted slope disagreement less than $27 \mu\text{Hz}$. After a duration of 5 min, a maximum Doppler of about 9 kHz was achieved.

Figure 15 clearly indicates that the modulated code data (PRN 1) were successfully passed through the PERFS prototype and tracked by the software GPS receiver. The measured Doppler resulting from the Doppler ramp PERFS agrees well with the commanded Doppler.

Figure 16 shows the estimated carrier-to-receiver noise density (C/N_0) of the tracked

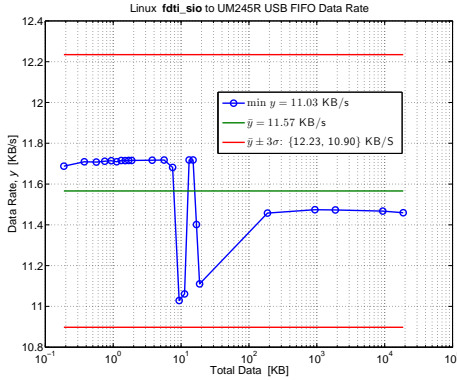


Figure 17. Maximum steady state data-rate for FTDI FT245R USB FIFO interface using standard Linux kernel v2.6 ftdi_sio driver.

signal, where $C/N_0 < 48$ dB-Hz for the duration of the run. The estimated C/N_0 is likely conservative due to clock jitter in the Universal Software Radio Peripheral (USRP).

The GPS receiver successfully tracked the coded GPS PRN 1 signal through-out the duration of the test.

V.E. USB Interface

The data rate results can be seen in Figure 17. The combination of the default VCP drivers and the FTDI FT245R chipset produce an average sustained data rate greater than 11 kB/s. This exceeds the expected minimum sustained data rate of 5 kB/s per device. In addition, the 3σ lower bound also exceeds the expected minimum sustained rate by a factor of 2.

VI. Conclusions

This work presents the concept, design, and performance of the first production unit of the Path Emulator for Radio Frequency Systems. The concept of a coherent PERFS network is presented and its operation is described. The initial characterization successfully demonstrates the ability to modulate S-band radio frequency signals exchanged between spacecraft that emulates the dynamic environment through which the radio frequency signals travel. The initial production unit's minimum range offset and estimated average Doppler resolution is determined. The Doppler resolution error is shown to increase with larger applied Doppler commands, while smaller applied Doppler commands meet the specified requirement.

This new hardware capability is necessary to enable realistic, real-time, closed-loop, hardware-in-the-loop simulations that include radio frequency ranging sensors for relative navigation. In addition, the development of the Crosslink Environment Simulator enables the concept of a coherent network of individual PERFS units.

Iterative development continues on the production PERFS to meet the requirements necessary to support maturation of the Inter-spacecraft Ranging and Alarm System for the Magnetospheric Multiscale mission.

Acknowledgments

The development of the Path Emulator for Radio Frequency Systems (PERFS) is supported by NASA's Office of Space Communications and Navigation (SCaN) and the Magnetospheric Multiscale (MMS) Mission.

References

- ¹Smith, D. and Colón, G., "Magnetospheric Multiscale Mission," <http://stp.gsfc.nasa.gov/missions/mms/mms.htm>, Accessed January 23, 2007.
- ²Gendreau, K. C., Cash, W. C., Gorenstein, P., Windt, D. L., Kaaret, P., and Reynolds, C., "MAXIM: The Black Hole Imager," *Proceedings of the SPIE*, Vol. 5488, 2004, pp. 394–402.
- ³White, N. E. and Newman, P., "Micro-Arcsecond X-ray Imaging Mission," 2007, <http://maxim.gsfc.nasa.gov/>, Accessed January 23, 2007.
- ⁴Leisawitz, D., "Submillimeter Probe of the Evolution of Cosmic Structure," <http://space.gsfc.nasa.gov/astro/specs/>, Accessed January 23, 2007.
- ⁵Carpenter, K., "Stellar Imager," <http://hires.gsfc.nasa.gov/~si/>, Accessed January 23, 2007.
- ⁶European Space Agency, "Darwin Mission," <http://tinyurl.com/86n5h>, Accessed January 23, 2007.
- ⁷Swedish Space Corporation, "Prisma Mission," <http://tinyurl.com/2p4z3u>, Accessed June 14, 2007.
- ⁸European Space Agency, "Proba-3 Mission," <http://tinyurl.com/34apzm>, Accessed June 14, 2007.
- ⁹Leitner, J., "A Hardware-in-the-Loop Testbed for Spacecraft Formation Flying Applications," *Proceedings of the IEEE Aerospace Conference*, Vol. 2, 2001, pp. 615–620.
- ¹⁰Naasz, B. J., Burns, R. D., Gaylor, D., and Higinbotham, J., "Hardware-in-the-Loop Testing of Continuous Control Algorithms for a Precision Formation Flying Demonstration Mission," *18th International Symposium on Space Flight Dynamics*, 2004.
- ¹¹Mitchell, J. W. and Luquette, R. J., "Recent Developments in Hardware-in-the-Loop Formation Navigation and Control," *NASA Goddard Flight Mechanics Symposium*, 2005.
- ¹²Mankins, J. C., "Technology Readiness Levels," 1995, <http://www.hq.nasa.gov/office/codeq/tr1/>, Accessed May 23, 2007.
- ¹³Wikipedia, "Technology Readiness Level," <http://tinyurl.com/3bpug3>, Accessed May 23, 2007.
- ¹⁴Grambling, C., "Orbit and Navigation Level 2 Requirements, Processes, and Operations Concept Document," NASA Goddard Space Flight Center, Solar Terrestrial Proves Program, MMS Mission, MMS-461-OPS-0002.
- ¹⁵NASA GSFC Mission Engineering and Systems Analysis Division, "GEONS Open Architecture Solutions for Onboard Orbit Determination in any Orbit," 2005, <http://geons.gsfc.nasa.gov/>, Accessed January 23, 2007.
- ¹⁶Hunt, C., Smith, C., and Burns, R., "Development of a Crosslink Channel Simulator," *Proceedings of the IEEE Aerospace Conference*, Vol. 2, 2004, pp. 1322–1328.
- ¹⁷Mitchell, J. W., Zakar, D. M., Burns, R. D., and Luquette, R. J., "A Message Oriented Middleware for a Soft Real-Time Hardware-in-the-Loop Spacecraft Formation Flying Testbed," *AIAA Modeling and Simulation Technologies Conference*, 2006.
- ¹⁸Mitchell, J. W., Baldwin, P. J., Kurichh, R., Naasz, B. J., and Luquette, R. J., "Characterization of a Prototype Radio Frequency Space Environment Path Emulator for Evaluating Spacecraft Ranging Hardware," *AIAA Guidance, Navigation, & Control Conference*, 2007.
- ¹⁹Maral, G. and Bousquet, M., *Satellite Communication Systems (Systems, Techniques and Technology)*, John Wiley & Sons, 2nd ed., 1994.
- ²⁰Taylor, B. N. and Mohr, P. J., "CODATA Value: speed of light in vacuum," 2006, <http://physics.nist.gov/cgi-bin/cuu/Value?c>, Accessed April 18, 2008.
- ²¹Thornton, S. T. and Rex, A., *Modern Physics for Scientists and Engineers*, Brooks/Cole, Thompson Learning, 2nd ed., 2002.
- ²²Nelson, R. A., "Relativistic Effects in Satellite Time and Frequency Transfer and Dissemination," *ITU Handbook on Satellite Time and Frequency Transfer and Dissemination*, Geneva, 2004, in press.
- ²³Davies, R. S., "Communications Architecture," *Space Mission Analysis and Design*, edited by J. R. Wertz, Kluwer Academic Publishers, 1991, pp. 441 – 90.
- ²⁴Press, W. H., Teukolsky, S. A., Vetterling, W. T., and Flannery, B. P., *Numerical Recipes in C: The*

Art of Scientific Computing, Cambridge University Press, 2nd ed., 1992.

²⁵Heckler, G. W. and Garrison, J. L., “Architecture of a reconfigurable software receiver,” *Institute of Navigation GNSS*, 2004.

²⁶Heckler, G. W., “Exploring GPS with Software Defined Radio,” July 2008, <http://www.gps-sdr.com/>.

²⁷Future Technology Devices International Ltd., “Virtual COM Port Drivers,” 2007, <http://www.ftdichip.com/Drivers/VCP.htm>, Accessed January 23, 2007.